Title

Metabolic fate of glucose in rats with traumatic brain injury and pyruvate or glucose treatments: A NMR spectroscopy study

Authors

Shijo, Katsunori
Sutton, Richard L
Ghavim, Sima S
et al.

Publication Date

2017

DOI

10.1016/j.neuint.2016.11.014

Peer reviewed

HHS Public Access

Author manuscript

Neurochem Int. Author manuscript; available in PMC 2018 January 01.

Published in final edited form as:

Neurochem Int. 2017 January ; 102: 66–78. doi:10.1016/j.neuint.2016.11.014.

Metabolic fate of glucose in rats with traumatic brain injury and pyruvate or glucose treatments: A NMR spectroscopy study

Katsunori Shijo[a,1], **Richard L. Sutton**[a], **Sima S. Ghavim**[a], **Neil G. Harris**[a], and **Brenda L. Bartnik-Olson**[b,*]

[a]Brain Injury Research Center, Department of Neurosurgery, David Geffen School of Medicine at UCLA, Los Angeles, Box 956901, CA, USA

[b]Department of Radiology, Loma Linda University School of Medicine, Loma Linda, CA, USA

Abstract

Administration of sodium pyruvate (SP; 9.08 μmol/kg, i.p.), ethyl pyruvate (EP; 0.34 μmol/kg, i.p.) or glucose (GLC; 11.1 μmol/kg, i.p.) to rats after unilateral controlled cortical impact (CCI) injury has been reported to reduce neuronal loss and improve cerebral metabolism. In the present study these doses of each fuel or 8% saline (SAL; 5.47 nmoles/kg) were administered immediately and at 1, 3, 6 and 23 h post-CCI. At 24 h all CCI groups and non-treated Sham injury controls were infused with [1,2 ^{13}C] glucose for 68 min ^{13}C nuclear magnetic resonance (NMR) spectra were obtained from cortex + hippocampus tissues from left (injured) and right (contralateral) hemispheres. All three fuels increased lactate labeling to a similar degree in the injured hemisphere. The amount of lactate labeled via the pentose phosphate and pyruvate recycling (PPP + PR) pathway increased in CCI-SAL and was not improved by SP, EP, and GLC treatments. Oxidative metabolism, as assessed by glutamate labeling, was reduced in CCI-SAL animals. The greatest improvement in oxidative metabolism was observed in animals treated with SP and fewer improvements after EP or GLC treatments. Compared to SAL, all three fuels restored glutamate and glutamine labeling via pyruvate carboxylase (PC), suggesting improved astrocyte metabolism following fuel treatment. Only SP treatments restored the amount of [4 ^{13}C] glutamate labeled by the PPP + PR pathway to sham levels. Milder injury effects in the contralateral hemisphere appear normalized by either SP or EP treatments, as increases in the total pool of ^{13}C lactate and labeling of lactate in glycolysis, or decreases in the ratio of PC/PDH labeling of glutamine, were found only for CCI-SAL and CCI-GLC groups compared to Sham. The doses of SP, EP and GLC examined in this study all enhanced lactate labeling and restored astrocyte-specific PC activity but differentially affected neuronal metabolism after CCI injury. The restoration of astrocyte metabolism by all three fuel treatments may partially underlie their abilities to improve cerebral glucose utilization and to reduce neuronal loss following CCI injury.

*Corresponding author. Department of Radiology, Loma Linda University Medical Center, 11234 Anderson Street, Room B623, Loma Linda, CA, 92354, USA.

[1]Current address: Department of Neurological Surgery, Nihon University School of Medicine, 30-1 Oyaguchi-kamimachi, Itabashi-ku, Tokyo 173-8610, Japan.

Disclosure statement

None of the authors have conflicting financial interests relevant to this work.

Keywords

Controlled cortical impact; Ethyl pyruvate; Glucose; Oxidative metabolism; Pentose phosphate pathway; Sodium pyruvate

1. Introduction

Traumatic brain injury (TBI) is well known to result in a cascade of inter-related physiological and biochemical reactions that alter cerebral metabolic pathways and impact the ability of injured cells to produce sufficient energy. Acute glutamate release and ionic fluxes are thought to underlie early increases in cerebral metabolic rates for glucose and aerobic glycolysis leading to elevated levels of lactate and reductions in extracellular glucose (Alessandri et al., 1999; Bartnik et al., 2005; Chen et al., 2000; Dhillon et al., 1997; Fukushima et al., 2009; Katayama et al., 1990, 1995; Kawamata et al., 1992; Kawamata et al., 1995; Krishnappa et al., 1999; Lee et al., 1999; Marklund et al., 2006; Nilsson et al., 1990; Palmer et al., 1993; Rose et al., 2002; Sunami et al., 1989; Sutton et al., 1994; Yoshino et al., 1991). TBI-induced mitochondrial dysfunctions will not only reduce oxidative metabolism, but increase free radical production and oxidative/nitrosative stress (Hall et al., 1993, 2004; Marklund et al., 2001; Tavazzi et al., 2005; Verweij et al., 1997; Xiong et al., 1997). The oxidative/nitrosative stress after TBI can modify many metabolic enzymes including glyceraldehyde-3-phosphate dehydrogenase (GAPDH) or the pyruvate dehydrogenase complex (PDH) (Humphries and Szweda, 1998; Kochanek et al., 2006; Opii et al., 2007; Ralser et al., 2007; Tabatabaie et al., 1996; Xing et al., 2009, 2012). In conjunction with zinc release, oxidative/nitrosative stress post-TBI can activate poly(ADP-ribose) polymerases (PARP) leading to reductions in nicotinamide adenine dinucleotide (NAD^+) (Besson et al., 2003; Clark et al., 2007; Hellmich et al., 2007; Laplaca et al., 1999; Satchell et al., 2003; Sheline et al., 2000; Suh et al., 2000, 2006) and inhibition of hexokinase (Andrabi et al., 2014). Because NAD^+ is a co-factor for GAPDH and lactate dehydrogenase (LDH), both glycolysis and conversion of lactate to pyruvate [pyruvate + NADH $\leftrightarrow$ lactate + NAD^+] for use in the tricarboxylic acid (TCA) cycle may become inhibited after TBI. The effects of injury on metabolic enzymes no doubt contribute to the development of cerebral metabolic depression following TBI (Bergsneider et al., 2000; Dunn-Meynell and Levin, 1997; Hovda et al., 1991; Prins and Hovda, 2009; Sutton et al., 1994; Yoshino et al., 1991).

Our laboratory has recently reported that administration of exogenous fuels early after experimental TBI can attenuate the reductions in cerebral glucose utilization, as measured by ^{14}C 2-deoxyglucose autoradiography, that occur by 24 h post-injury. Specifically, injections (i.p.) of high dose glucose (GLC; 11.1 μmol/kg), sodium pyruvate (SP; 9.08 μmol/kg) or ethyl pyruvate (EP; 0.34 μmol/kg) in the first 6 h after unilateral controlled cortical impact (CCI) injury were all found to improve cortical and subcortical glucose utilization by 24 h (Moro et al., 2013, 2016). In addition, each of these fuels, at the reported doses, were neuro-protective and beneficial in terms of behavioral outcome (Moro et al., 2013, 2016; Moro and Sutton, 2010; Shijo et al., 2015). However, the specific metabolic pathways potentially mediating these effects are unknown, and it remains unclear if these

exogenous fuel treatments alter metabolic pathways beyond the uptake of glucose. Using ^{13}C NMR spectroscopy, we previously reported injury-induced increases in the amount of glucose metabolized via the PPP, elevated glycolysis and alterations to the neuron and astrocyte TCA cycles and glutamate-glutamine cycle at 3.5 and 24 h after CCI injury (Bartnik et al., 2005). Using a similar design, we hypothesized that the addition of GLC, SP, or EP during the first 24 h post injury would reduce glucose metabolism through the PPP, indicating a reduction in oxidative stress. In addition, we hypothesized that these fuels would improve neuronal oxidative metabolism, consistent with our earlier observations of enhanced neuronal survival (Moro et al., 2013, 2016).

2. Materials and methods

2.1. Subjects

Adult male Sprague-Dawley rats (305 ± 2.3 g) from Charles River Breeding Labs (Hollister, CA) were used as experimental subjects (n = 50). Upon arrival, rats were pair housed and acclimated for 1–2 weeks to our standard temperature and lighting conditions (70–76 °F, 30–70% humidity, room lights on 06:00–18:00), with food (Teklad 7904) and tap water available *ad libitum*. All experimental procedures were approved by the UCLA Chancellor's Committee for Animal Research.

2.2. Surgical procedures

At 60–65 days of age, animals were anesthetized with isoflurane (2.0–2.5% in 100% O_2, 2.0 ml/min flow rate) and placed into a stereotaxic frame (Kopf Instruments, Tujunga, CA) with the head positioned in a horizontal plane with respect to the interaural line. During all surgical procedures, body temperature was maintained at 37 ± 1 °C using a thermostatically controlled heating pad (Harvard Apparatus, Holliston, MA). All surgical procedures were performed under aseptic conditions, and have been previously described in detail (Fukushima et al., 2009; Moro and Sutton, 2010; Sutton et al., 1993). In brief, following a midline incision, the skin, fascia and temporal muscle were reflected. Animals receiving CCI were subjected to a 6-mm diameter craniotomy over the left parietal cortex centered at 3 mm posterior and 3.5 mm lateral to bregma. An electronically controlled, small bore, dual-stroke, pneumatic piston cylinder with a 40-mm stroke (Hydraulics Control, Inc., Emeryville, CA) was mounted onto a stereotaxic micro-manipulator, allowing for precise control of the impact site and depth of tissue compression. The piston cylinder was angled 20° away from vertical, enabling the flat, circular impactor tip (5-mm diameter) to be perpendicular to the surface of the brain at the site of injury. A moderate severity of CCI injury was induced, using 20 psi (~2.2 m/s velocity) and 2.0 mm depth of tissue compression for 250 msec. Control (Sham injury) rats underwent similar procedures to control for surgical stress and duration of anesthesia, but did not receive craniotomy or any impact. After the scalp was sutured closed, bupivacaine (0.1–0.14 mg/kg, s.c.) was injected around the incision site, the rats were placed in a heated recovery cage (36.0–38.0 °C) until ambulatory, and then returned to their home cages.

Brain tissue swelling within the first 1–2 min post-CCI was recorded on surgical records as mild, mild-to-moderate, moderate, moderate-to-severe, or severe. These descriptors were

assigned rating scores of 0.5, 1.0, 1.5, 2.0 and 2.5, respectively, and the average rating for each CCI group was calculated as a measure of the initial injury severity. All animals were weighed prior to surgery and the day after surgery, with change in body weight used as a secondary measure of surgical and treatment effects.

This injury results in an approximately 35% loss of the cortical mantle at 2 weeks post-injury (Fukushima et al., 2009). Given the rate of atrophy in this model (Chen et al., 2003) we estimate that approximately 25% of the cortical tissue is necrotic at 1 day post-injury, the time-point used in the current study.

2.3. Experimental design and treatments

Fig. 1 shows the overall timeline of the post-surgical experimental procedures. Prior to surgery animals were randomly assigned to one of five groups (n = 10/group). Sham control animals did not receive injections post-surgery. Rats with CCI injury received intraperitoneal (i.p.) injections immediately after induction of CCI (denoted as 0 h) and at 1, 3, 6 and 23 h post-injury (Fig. 1). One CCI group was injected with 8% saline (CCI-SAL; cited as osmolarity control for GLC (Sugimori et al., 1996). SP (P2256: Sigma Aldrich, Saint Louis, MO, USA), EP (E47808: Sigma Aldrich) and GLC (G8270, Sigma Aldrich) were prepared at concentrations of 400, 16 or 500 mg/ml, respectively, in either 0.1 M phosphate buffered saline (Na_2HPO_4, S0876: Sigma Aldrich; SP and EP) or in 0.9% saline (for GLC). Doses administered with each injection were SAL = 5.47 nmoles/kg (0.32 mg/kg), SP = 9.08 μmol/kg (1000 mg/kg), EP = 0.34 μmol/kg (40 mg/kg), and GLC = 11.1 μmol/kg (2 g/kg) as previously described (Fukushima et al., 2009; Moro et al., 2013, 2016; Shijo et al., 2015). The calculated osmolarity of the injected solutions was 8% SAL (274 mOsmol/L), SP (445 mOsmol/L), EP (400 mOsmol/L), GLC (316 mOsmol/L). All solutions were filtered (0.22 μm) just prior to injection.

2.4. [1,2 $^{13}C_2$] glucose infusion

At 22 h after their initial surgery (Fig. 1), rats were anesthetized and the right femoral artery and vein were cannulated with PE-50 tubing, as previously described (Bartnik et al., 2007; Bartnik-Olson et al., 2010). The scalp incision was re-opened, the skull was dried, and the dorsal surface of the skull including the craniotomy site was covered with dental acrylic (to prevent overheating and herniation of cortical tissue through the craniotomy during microwave irradiation). Bupivacaine (0.1–0.14 mg/kg, s.c.) was infiltrated into the femoral and cranial incision sites and animals were restrained on a cardboard plank immediately after removal of isoflurane anesthesia.

At 24 h post-injury awake, lightly restrained animals were given an intravenous infusion of [1,2 $^{13}C_2$] glucose (Cambridge Isotope Laboratories, Andover, MA, USA) in sterile water (Fig. 1). The infusion protocol, per 350 g body weight, began with a bolus injection of 225 μmol followed by 150 μmol given in exponentially decreasing amounts over the next 8 min, until a final constant infusion rate of 16.67 μmol/min was reached and maintained for 1 h (Bartnik-Olson et al., 2010) (Fig. 1).

2.5. Blood sampling

Arterial blood samples (~0.1 mL) were taken prior to infusion (baseline), after 15 min of infusion, and just before the end of the ^{13}C glucose infusion (67 min) to measure blood pH, partial pressure of oxygen (pO_2), oxygen saturation (O_2 Sat), partial pressure of carbon dioxide (pCO_2), and bicarbonate (HCO_3) (Siemens Rapidpoint 340, Healthcare Diagnostics Inc, Plainfield, IN; Fig. 1). Aliquots (~0.1 mL) of all three blood sample were centrifuged (14,000 g for 5 min) and plasma glucose and lactate concentrations were measured using a 2700 Select Biochemistry Analyzer (YSI Inc., Yellow Springs, OH). A Bligh-Dyer (Bligh and Dyer, 1959) lipid and metabolite extraction was performed on plasma (0.25 mL) from an additional arterial blood sample (0.6 mL) collected at 67 min. The sample was placed into a SuperSpin microtube (VWR Cat.No. 2170-038) with methanol (0.5 mL), chloroform (0.5 mL), and distilled water (0.25 mL). After mixing, this sample was centrifuged (13,000 g for 20 min at 4 °C) to produce a three phase solution: aqueous metabolites, proteins, and hydrophobic lipids. All three phases were collected into separate glass vials and dried at room temperature under N_2 gas flow. The dried aqueous, protein, and lipid pellets were weighed and stored at −70 °C until use; the aqueous sample was used for determination of plasma ^{13}C-labeled glucose and lactate concentrations. The total volume of whole blood removed at each sampling time point was approximately 0.8 mL.

2.6. Euthanasia, tissue fixation and metabolic extraction

At the end of the ^{13}C-glucose infusion all animals were rapidly anesthetized with isoflurane (4% in 100% O_2 with a1.5–2.0 L/min flow rate) and euthanized via a focused beam of microwave irradiation (3.5 kW, 2.75–3.00 s) to the head (Thermex-Thermatron Model 4104 Microwave Fixation System, Louisville, KY; Fig. 1). The brains were removed and dissected to collect an ~8 × 8 mm section of the right (contralateral) and left cortex (±4.0 mm from injury center, from midline to the rhinal fissure) and the underlying hippocampus. Tissue samples were weighed in a tared SuperSpin microtube (VWR), and then processed for aqueous metabolites and lipid extraction using the Bligh-Dyer technique (Bligh and Dyer, 1959). This extraction method results in a higher (7–15%) metabolite yield versus perchloric acid (PCA) extraction but with lower protein content in the remaining pellet (Le Belle et al., 2002). As a result, metabolite levels normalized to this lower protein concentration will result in higher metabolite concentrations compared to studies using a PCA extraction technique. Methanol and chloroform were added in the ratio of 1:2:1 tissue:methanol:chloroform (100 μl/mg tissue) and the samples were sonicated (20 pulses; Sonic Dismembrator; Fisher Scientific, Pittsburgh, PA). Additional chloroform and distilled water were added to the samples in a 1:1 ratio to obtain a final ratio of 1:2:2:1 tissue:methanol:-chloroform:water (Harris et al., 1996; Miccheli et al., 1988) and the resulting emulsion was centrifuged at 13,000 g for 20 min at 4 °C to produce a three phase solution: aqueous metabolites, proteins, and hydrophobic lipids. All three phases were collected into separate glass vials and dried at room temperature under N_2 gas flow. The dried aqueous, protein, and lipid pellets were weighed and stored at −70 °C until use. The dried aqueous extracts were reconstituted in 0.6 mL deuterium oxide (D_2O; 99.9% D) containing 0.05–0.075% weight sodium 3-(trimethylsilyl) propionate (TSP) immediately before spectroscopic analysis.

2.7. Protein determination

Protein pellets were solubilized in a 9X volume of 1 M NaOH and the protein content was measured using the Bio-Rad protein assay on a SPECTRAmax 190 microplate spectrophotometer (Molecular Devices, Sunnyvale, CA) at a wavelength of 595 nm.

2.8. NMR spectroscopy acquisition and analysis

^{13}C NMR spectra were obtained on a Bruker AVANCE 500 MHz spectrometer. Proton decoupled ^{13}C spectra were acquired using a 70° pulse angle, 1.1-sec acquisition time, 3-sec recycle delay, and a 12 ppm spectral width. Waltz 16 broad band decoupling was used during the acquisition of the ^{13}C spectra to avoid nuclear Over-hauser enhancement effects. The number of acquisitions was typically 13,000–14,000.

Chemical shifts were assigned relative to TSP and by comparison to previously published values (Cruz and Cerdan,1999; Govindaraju et al., 2000). All peaks were integrated using NUTS (Acorn NMR Inc., Livermore, CA, USA), quantified using TSP as an internal standard (Badar-Goffer et al., 1990) and normalized to the total protein content of each sample. The total amount (nmol/mg protein) of ^{13}C labeled glucose, lactate, glutamate, glutamine, GABA, and aspartate was calculated as the sum of all detected ^{13}C isotopomers: [3 ^{13}C] and [2,3 $^{13}C_2$] lactate; [4,5 $^{13}C_2$], [2,3 $^{13}C_2$], [1,2 $^{13}C_2$], [4 ^{13}C], [1 ^{13}C] and [5 ^{13}C] glutamate and glutamine; [1,2 $^{13}C_2$], [3,4 $^{13}C_2$] and [2 ^{13}C] GABA and aspartate. The ^{13}C percent enrichment of plasma glucose and lactate was calculated by dividing the concentration of plasma ^{13}C glucose and ^{13}C lactate, measured by ^{13}C NMR spectroscopy (mM/L), by the plasma glucose and lactate concentration obtained by YSI (mM/L) multiplied by 100.

2.9. Labeling pattern following [1,2 $^{13}C_2$] glucose infusion

Fig. 2 shows a simplified scheme of the ^{13}C labeling of metabolites following an infusion of [1,2 $^{13}C_2$] glucose. The metabolism of [1,2 $^{13}C_2$] glucose through glycolysis leads to [2,3 $^{13}C_2$] pyruvate, which can be reduced to [2,3 $^{13}C_2$] lactate or transaminated to [2,3 $^{13}C_2$] alanine. The [2,3 $^{13}C_2$] pyruvate can enter the TCA cycle through PDH as [1,2 $^{13}C_2$] acetyl CoA leading to the formation of [1,2 $^{13}C_2$] citrate and after a few steps α-[4,5 $^{13}C_2$] ketoglutarate, which can exit the TCA cycle to produce [4,5 $^{13}C_2$] glutamate, [4,5 $^{13}C_2$] glutamine, and [1,2 $^{13}C_2$] GABA. If the α-[4,5–$^{13}C_2$] ketoglutarate remains in the TCA cycle the ^{13}C labeled carbon skeletons will be scrambled at succinate resulting in equal amounts of [1,2 $^{13}C_2$] and [3,4 $^{13}C_2$] succinate, giving rise to [1,2 $^{13}C_2$] and [3,4 $^{13}C_2$] fumarate, malate, oxaloacetate and aspartate. In a second turn of the TCA cycle [1,2 $^{13}C_2$] and [3,4 $^{13}C_2$] oxaloacetate can condense with un-labeled acetyl CoA resulting in glutamate and glutamine labeled as either a doublet ([1,2 $^{13}C_2$]) or as a singlet ([3 ^{13}C]).

In astrocytes, the [2, 3 $^{13}C_2$] pyruvate from glycolysis can also be carboxylated by pyruvate carboxylase (PC), enter the TCA cycle as [2,3 $^{13}C_2$] oxaloacetate, which can condense with acetyl CoA to form [3,4 $^{13}C_2$] citrate. After a number of steps α-[2,3 $^{13}C_2$] ketoglutarate is formed, which can then give rise to [2,3 $^{13}C_2$] glutamate and glutamine. If [2,3 $^{13}C_2$] glutamine is transported from the astrocyte to glutamatergic or GABAergic neurons it can be converted to [2,3 $^{13}C_2$] glutamate or [3,4 $^{13}C_2$] GABA. If the ^{13}C label originating from PC

remains in the astrocyte TCA cycle for a second turn and condenses with unlabeled acetyl CoA, it will give rise to [3 ^{13}C] and [1,2 $^{13}C_2$] glutamate and glutamine; if transported to neurons, [3 ^{13}C] and [1,2 $^{13}C_2$] glutamate or [3 ^{13}C] and [4 ^{13}C] GABA will result.

The pyruvate recycling (PR) pathway represents a major cataplerotic pathway for the complete oxidation of glutamate and has been observed in astrocytes and to a lesser extent, neurons (reviewed in McKenna, 2013; Schousboe, 2015). In this process, [1,2 $^{13}C_2$] and [3,4 $^{13}C_2$] oxaloacetate or malate can exit the TCA cycle and be decarboxylated to [3 ^{13}C] or [1,2 $^{13}C_2$] pyruvate via phosphoenolpyruvate carboxykinase (PEPCK) and pyruvate kinase (PK) or malic enzyme (ME). The newly labeled (recycled) pyruvate can be converted to [1 ^{13}C] and [2 ^{13}C] acetyl CoA via PDH and enter the TCA cycle as [1 ^{13}C] and [2 ^{13}C] citrate leading to the labeling of [4 ^{13}C] glutamate/glutamine and [2 ^{13}C] GABA. In partial pyruvate recycling, the newly labeled pyruvate is converted to [3 ^{13}C] and [1,2 $^{13}C_2$] lactate.

[1,2 $^{13}C_2$] glucose can also be metabolized via the PPP, where one of the ^{13}C atoms is lost as $^{13}CO_2$ during the formation of [1 ^{13}C] ribulose-5-phosphate. In the oxidative branch of the PPP, 3 molecules of [1 ^{13}C] ribulose-5-phosphate are metabolized to form 1 molecule each of [1^{13}C] fructose-6-phosphate, [1,3 $^{13}C_2$] fructose-6-phosphate and unlabeled glyceraldehyde-3-phosphate. The [1 ^{13}C] and [1,3 $^{13}C_2$] labeled fructose-6-phosphate can reenter the glycolytic pathway where it is metabolized to [3 ^{13}C] and [1,3 $^{13}C_2$] pyruvate. Three molecules of [1,2 $^{13}C_2$] glucose will generate one molecule each of [3 ^{13}C] and [1,3 $^{13}C_2$] pyruvate and three molecules of unlabeled pyruvate, which can then be reduced to [3 ^{13}C] and [1,3 $^{13}C_2$] lactate, transaminated to [3 ^{13}C] and [1,3 $^{13}C_2$] alanine or enter the TCA cycle. If metabolized by PDH, both [3 ^{13}C] and [1,3 $^{13}C_2$] pyruvate are converted to [2 ^{13}C] acetyl CoA and enter the TCA cycle as [2 ^{13}C] citrate, leading to the formation of [4 ^{13}C] glutamate/glutamine and [2 ^{13}C] GABA. If metabolized by PC, [3 ^{13}C] and [1,3 $^{13}C_2$] pyruvate enter the TCA cycle as [3 ^{13}C] and [1,3 $^{13}C_2$] oxaloacetate, leading to the formation of [3 ^{13}C] glutamate/glutamine and GABA. In the non-oxidative branch of the PPP, ribulose-5-phosphate is converted to ribose-5-phosphate, an essential precursor for nucleotide synthesis. Because the labeling of biosynthetic compounds from the non-oxidative branch were too low to be measured, they were omitted from Fig. 2.

2.10. Metabolic pathway estimates

The metabolism of [1,2 $^{13}C_2$] glucose leads to clear labeling patterns of lactate, glutamate, and glutamine in the first turn of the TCA cycle. In subsequent turns of the TCA cycle, isotopomers from different metabolic pathways can lead to similar labeling patterns (Fig. 2), thus only isotopomers originating in the first turn of the TCA cycle were used to calculate estimates of metabolic pathway activity.

Activity of both the PPP + PR pathway can result in the labeling of [3 ^{13}C] lactate, [4 ^{13}C] glutamate and [4 ^{13}C] glutamine. Calculating the [3 ^{13}C] lactate/[2,3 $^{13}C_2$] lactate ratio provides an estimate of the relative contribution of the PPP + PR pathway and glycolysis to lactate labeling. This approach makes no assumptions regarding the relative contribution of either the PPP or PR pathway nor does it account for any differences in pathway flux between cell types or the loss of labeled lactate to the TCA cycle or exported to the bloodstream. Thus any increase in this ratio could reflect an increase in glucose metabolism

via the PPP, an increase in PR activity, or a decrease in glycolysis. The values presented in Table 3 and Supplemental Table 2 are the minimal values for this ratio. These values would be 1.5 fold higher if the PPP was the sole contributor to [3 ^{13}C] lactate labeling, as all values associated with the PPP must be multiplied by 1.5 to adjust for the fact that 3 molecules of [1,2 $^{13}C_2$] glucose metabolized by the PPP would give rise to 2 labeled and one unlabeled molecule of lactate whereas the same number of [1,2 $^{13}C_2$] glucose molecules metabolized via glycolysis would give rise to 3 molecules of labeled lactate (Morken et al., 2014).

Similarly, calculating the [4 ^{13}C] glutamate/[4,5 $^{13}C_2$] glutamate (or glutamine) ratio provides an estimate of the relative contribution of the PPP + PR pathway and oxidative metabolism via PDH to glutamate or glutamine labeling. Again this approach does not assume the relative contribution of either pathway to glutamate or glutamine ^{13}C labeling. An increase in this ratio would reflect an increased contribution of pyruvate labeled via the PPP or PR pathway or a decrease in the contribution of glycolysis-derived pyruvate to glutamate or glutamine labeling. A shift in the contribution of the PPP + PR pathway to lactate (PPP + PR lactate), glutamate (PPP + PR glutamate) or glutamine (PPP + PR glutamine) labeling following injury and/or fuel treatment would indicate changes in pyruvate metabolism.

The contribution of astrocytes to glutamate (or glutamine) labeling can be derived from the PC/PDH ratio, which estimates the contribution of the astrocytic anaplerotic pathway (PC) relative to PDH activity which is found in both the neuron and astrocyte compartments. The PC/PDH ratio was calculated using the formula [2,3 $^{13}C_2$] glutamate (or glutamine)/ [4,5 $^{13}C_2$] glutamate (or glutamine) [reviewed in (Sonnewald and Rae, 2010)]. An increase in the PC/PDH ratio reflects either an increase in PC activity or a decrease in PDH activity. The PC/PDH ratio was calculated for both glutamate and glutamine to explore shifts in the compartmentation of metabolic pathways following injury and fuel treatment.

2.11. Data exclusions and statistical analysis

Each animal produced three samples for NMR analysis: i) the plasma sample post- ^{13}C glucose infusion, ii) the left (injured) hemisphere tissue sample, and iii) the right (contralateral) hemisphere tissue sample. Spectra were excluded if a glucose peak was not detected in ^{13}C spectra of plasma or tissue samples, suggesting technical issues with the label infusion or sample preparation, or if the signal-to-noise ratio of a sample was too low to reliably detect metabolites of interest. These data exclusions led to the following sample sizes for left or right tissue samples: Sham (left n = 8, right n = 10); CCI-SAL (left n = 8, right n = 9); CCI-SP (left n = 8, right n = 10); CCI-EP (left n = 9, right n = 9); CCI-GLC (left n = 8, right n = 10). Plasma data remained in the biochemistry and NMR analysis (Table 1) if ^{13}C spectra from either the left or right tissue samples from that animal were used in the final analysis. Isotopomers for some metabolites were not detectable in all tissue samples, and in such cases the reduced sample size for any affected group is specified in the text.

Group data are expressed as the mean ± standard error of the mean (SEM). Statistical analysis was performed using SPSS software (version 22: SPSS Inc., Chicago, IL, USA). For blood samples, the pre-infusion data were first analyzed using one-way ANOVA. If no

Group effect was found, repeated measures one-way analysis of variance (ANOVA) was used to test for Group, Time and Group X Time effects, with Bonferroni post hoc comparisons to determine individual group (pre-versus 15 and 67 min post-infusion) differences. In cases where a pre-infusion Group effect was detected (pH, HCO_3, lactate), repeated measures one-way analysis of covariance (ANCOVA) was used to control for the effects of the pre-infusion pH, HCO_3, and lactate differences. Between groups differences in measures of injury severity and ^{13}C concentration of plasma or tissue metabolites were determined using one-way ANOVA with a post-hoc Bonferroni comparison to determine individual group differences at a significance level of $p < 0.05$.

3. Results

3.1. Indices of injury severity

Ratings of tissue swelling acutely post-injury did not differ significantly between the four CCI groups (1.78 ± 0.12, 1.70 ± 0.08, 1.83 ± 0.08 and 1.75 ± 0.08 for SAL, SP, EP and GLC, respectively). Body weight loss 24 h post-injury was significant in the CCI-SAL (−15.0 ± 3.3 gm), CCI-SP (−19.3 ± 2.8 gm), CCI-EP (−19.4 ± 2.5 gm), and CCI-GLC (−16.4 ± 1.9 gm) compared to Sham controls (0.8 ± 1.3 gm; p's < 0.001), but weight loss did not differ between CCI groups. These combined findings indicate similar injury severity for the CCI-SAL, CCI-SP, CCI-EP and CCI-GLC groups.

3.2. Blood, plasma, and tissue protein measurements

A repeated measures ANCOVA controlling for elevated pre-infusion pH and HCO_3 levels in the CCI-SP group compared to all others (p's < 0.001, Table 1) revealed a significantly higher pH and HCO_3 in the CCI-SP group at both 15 and 67 min after initiating the ^{13}C glucose infusion (p's < 0.001). There were no between group effects on baseline pO_2, O_2 saturation or pCO_2 (Table 1). Repeated measures ANOVA showed no significant effects on the pO_2, O_2 saturation or pCO_2 measures (Table 1).

Plasma glucose concentrations were similar between groups prior to the ^{13}C glucose infusion (Table 1). Repeated measures ANOVA showed no effect for Group or Group X Time. A significant effect for Time was due to increased plasma glucose concentrations at 15 min into the ^{13}C glucose infusion that declined toward pre-infusion levels by 67 min in all groups (p's < 0.001).

A significant effect of Group for plasma lactate was seen at baseline due to higher lactate levels in the CCI-GLC group compared to the CCI-SAL group ($p < 0.05$). A significant Group effect found with repeated measures ANCOVA when controlling for the pre-infusion lactate concentration, which was due to higher levels in CCI-SP compared to the CCI-EP group ($p < 0.001$) and higher levels in the CCI-GLC compared to the CCI-SAL and CCI-EP groups at 15 min (p's < 0.001).

The total amount of protein recovered in the left (injured) tissue samples were: Sham controls (23.9 ± 5.6 mg), CCI-SAL (22.1 ± 7.2 mg), CCI-SP (17.9 ± 2.8 mg), CCI-EP (15.6 ± 6.1 mg), and CCI-GLC (21.3 ± 4.3 mg) which did not differ between the groups.

3.3. ^{13}C enrichment of glucose and lactate in plasma

Despite the minor variations in blood chemistry among the groups, the ^{13}C enrichment of plasma glucose at 67 min after initiating the ^{13}C glucose infusion were not statistically different for Sham (13.0 ± 1.6), CCI-SAL (15.5 ± 1.4), CCI-SP (13.3 ± 2.4), CCI-EP (14.2 ± 1.2) and CCI-GLC (11.8 ± 1.0) groups. The ^{13}C enrichment of plasma lactate was not analyzed statistically, due to its detection in only 24% of the animals. The lactate enrichment was 2.3% in Sham controls (n = 1), 1.4% ± 0.44 in CCI-SP (n = 5), 1.8% in CCI-EP (n = 1), 2.0% ± 0.7 in CCI-GLC (n = 3), and was not detected in CCI-SAL animals. The absence of plasma lactate labeling could suggest that the contribution of peripheral glucose metabolism during the 60 min infusion was lower than ^{13}C NMR detectable limits.

3.4. ^{13}C metabolite labeling and metabolic pathway estimates in left (injured) hemisphere

The total amounts (nmol/mg protein) of ^{13}C labeled glucose, lactate, glutamate, glutamine, GABA and aspartate isotopomers in left (injured) tissue samples after [1,2 $^{13}C_2$] glucose infusion are shown in Fig. 3. The amounts of individual lactate, glutamate, and glutamine isotopomers in the left hemisphere metabolites are listed in Table 2 and the metabolic pathway data are shown in Table 3.

The amounts of ^{13}C glucose in the left (injured) brain tissue samples were significantly increased in all CCI groups compared to Sham controls (p's < 0.05; Fig. 3). The amounts of ^{13}C glucose were higher in the SP, EP and GLC treatment groups compared to the SAL-treated group but did not reach significance.

Both the total amount of ^{13}C labeled lactate isotopomers and the amount of [2,3 $^{13}C_2$] lactate labeled via glycolysis in the left-injured hemisphere were not increased above Sham control levels in the CCI-SAL group but were significantly increased after SP, EP or GLC treatment (p's < 0.001; Fig. 3, Table 2). These increases in lactate after SP treatment were significant compared to SAL-treated controls ($p < 0.001$). The amount of [3 ^{13}C] lactate labeled via the PPP + PR pathway was significantly increased in all CCI groups compared to Sham controls (n = 4; p's < 0.001) and did not differ significantly between the CCI groups (Table 2).

The ratio of lactate labeled via the PPP + PR pathway relative to glycolysis gives an estimate of the combined contribution of the PPP and PR pathway to lactate synthesis. In the CCI-SAL group this ratio was significantly higher compared to Sham controls (n = 4; $p < 0.001$, Table 3), owing to an increase in [3 ^{13}C] lactate labeling. Although the [3 ^{13}C]/[2,3 $^{13}C_2$] lactate ratio was significantly reduced with fuel treatments (p's < 0.01 compared to CCI-SAL), this was the result of increased [2,3 $^{13}C_2$] lactate labeling and not reduced [3 ^{13}C] lactate labeling (Tables 2 and 3) indicating that the injury-induced increase in the contribution of the PPP + PR pathway to lactate labeling was unaffected by fuel treatment.

The total amount of all ^{13}C glutamate isotopomers in left-injured brain samples was significantly reduced in all four CCI groups compared to Sham controls (p's < 0.001 for SAL, EP and GLC; $p < 0.05$ for SP). Among CCI groups, the amounts were highest in the SP group although this was not significant (Fig. 3). The amount of [4,5 $^{13}C_2$] glutamate that was labeled via PDH in the first turn of the TCA cycle was significantly reduced from

Shams in all CCI groups (p's < 0.01) with exception of CCI-SP, which remained similar to Shams. The amount of [4,5 $^{13}C_2$] glutamate labeling in the CCI-SP group was also significantly higher than the amount in the CCI-GLC group ($p < 0.05$; Table 2). Glutamate labeled in the second turn of the TCA cycle ([1,2 $^{13}C_2$]), was significantly reduced to the same extent in all four of the CCI injury groups compared to Sham levels (p's ≤ 0.001; Table 2).

The amount of [2,3 $^{13}C_2$] glutamate labeled via PC was significantly lower than Sham values in the CCI-SAL ($p < 0.001$) and CCI-GLC ($p < 0.01$) groups, but not in the CCI-SP or CCI-EP groups, although this PC-derived glutamate did not differ significantly among the four CCI groups (Table 2). The ratio of glutamate labeled via PC relative to PDH was not different in any of the CCI groups compared to Sham, although the PC/PDH glutamate ratio for CCI-EP was significantly higher than that for CCI-SAL ($p < 0.05$; Table 3) due to reduced amounts of [2,3 $^{13}C_2$] (Table 2).

The amount of [4 ^{13}C] glutamate, labeled in the PPP + PR pathway, was significantly decreased in the CCI-SAL group compared to Sham ($p < 0.05$). In contrast, the amount of [4 ^{13}C] glutamate in the CCI-SP group was significantly higher compared to all other CCI groups (p's ≤ 0.001; Table 2). The contribution of the PPP + PR pathway to glutamate labeling was significantly higher in the CCI-SP group compared to Sham ($p = 0.01$), CCI-SAL ($p = 0.005$) and CCI-EP ($p < 0.005$) groups but not compared to CCI-GLC (Table 3) and was due to a non-significant increase in [4 ^{13}C] glutamate labeling (Table 2).

As shown in Fig. 3, the total amount of all ^{13}C labeled glutamine isotopomers was significantly reduced below Sham levels in all CCI groups (p's < 0.001), with the exception of CCI-SP. The total amount of ^{13}C glutamine in the CCI-SP group was significantly higher than for CCI-SAL ($p = 0.01$) and CCI-EP ($p = 0.005$), but not CCI-GLC ($p = 0.08$). In the CCI-SP or CCI-GLC groups, the amount of [4,5 $^{13}C_2$] glutamine labeled via PDH was not significantly different from Shams whereas the relative amount of [4,5 $^{13}C_2$] glutamine in the CCI-SAL and CCI-EP groups was significantly lower than Sham (p's < 0.005; Table 2). Higher amounts of [4,5 $^{13}C_2$] glutamine were found in the CCI-SP group compared to SAL and EP (p's < 0.01) treatments, and for CCI-GLC compared to CCI-SAL ($p < 0.05$). The amount of [1,2 $^{13}C_2$] glutamine labeled in the second turn of the TCA cycle was significantly lower in all four of the CCI groups compared to Sham (p's < 0.001), and did not differ significantly between the CCI groups (Table 2).

The amount of [2,3 $^{13}C_2$] glutamine labeled via PC was significantly reduced in the CCI-SAL group compared to the Sham and the CCI-SP groups (p's < 0.01) but did not differ between Sham and CCI-SP, CCI-EP or CCI-GLC groups (Table 2). The ratio of glutamine labeled via PC relative to PDH did not differ between any of the experimental groups (Table 3), however labeling of both [2,3 $^{13}C_2$] and [4,5 $^{13}C_2$] glutamine was reduced in the CCI-SAL group (Table 2).

The amount of [4 ^{13}C] glutamine labeled via the PPP + PR pathway was detectable in only 3 Sham, 6 CCI-SAL, 8 CCI-SP, 4 CCI-EP and 7 CCI-GLC animals and did not differ significantly from Sham in any CCI groups. However, the amounts measured in the CCI-

SAL group were significantly reduced compared to the CCI-GLC group ($p < 0.01$; Table 2). The contribution of the PPP + PR pathway to glutamine labeling did not differ between any of the experimental groups (Table 3).

Similar to glutamate, the total pools of ^{13}C labeled GABA and of ^{13}C aspartate in left-injured brain tissue samples were significantly reduced from Sham control values in all CCI groups (p's < 0.01; Fig. 2), with no effect of fuel treatment.

3.5. ^{13}C metabolite labeling and metabolic pathway estimates in right (contralateral) hemisphere

The total amounts of ^{13}C labeled glucose and lactate isotopomers as well as the amount of lactate derived via glycolysis were all significantly increased in brain tissue samples contralateral to CCI injury in the CCI-SAL and the CCI-GLC group compared to Shams (p's < 0.05; Supplemental Fig. 1). The total pool of ^{13}C labeled glucose was also higher in the CCI-GLC group compared to the CCI-EP group ($p < 0.05$). PPP + PR pathway-labeled [3 ^{13}C] lactate was significantly increased above Sham ($n = 8$) in the CCI-GLC group alone ($n = 5$; $p = 0.01$; Supplemental Table 1). There were no group differences in the contribution of the PPP + PR pathway to lactate labeling in the contralateral hemisphere (Supplemental Table 2).

There were no group differences in the total amount of ^{13}C labeled glutamate isotopomers and any individual glutamate isotopomer or metabolic pathway estimate in right tissue samples (Supplemental Fig. 1, Supplemental Tables 1 and 2).

The total amount of all ^{13}C labeled glutamine isotopomers did not differ between groups (Supplemental Fig. 1). However, glutamine labeled via PC was significantly reduced in the CCI-SAL group with a concomitant decrease in the PC/PDH ratio (p's ≤ 0.05; Supplemental Tables 1 and 2). Other effects in the right hemisphere were fuel specific, as CCI-GLC had increases in the amounts of [4,5 $^{13}C_2$] glutamine (via PDH in the first turn of the TCA cycle) compared to CCI-SP and CCI-EP (p's < 0.05) and increases in the amounts of [1,2 $^{13}C_2$] glutamine (second turn of the TCA cycle) compared to Sham controls and CCI-EP (p's < 0.05; Supplemental Table 2). In addition, the glutamine PC/PDH ratio was significantly reduced in the CCI-GLC group compared to Sham, CCI-SP and CCI-EP groups (p's ≤ 0.001; Supplemental Table 2).

4. Discussion

The primary aim of this study was to determine the effect of neuroprotective biofuels on glucose metabolism in the injured hemisphere 24 h following a unilateral CCI injury. The main findings are summarized in Fig. 4. The current results show that (1) treatments with EP, SP and GLC all increased lactate labeling to a similar degree, (2) lactate labeling via the PPP + PR pathway was increased by CCI injury and treatment with SP, EP, and GLC did not ameliorate this, (3) all fuel treatments prevented the injury-induced reduction in oxidative metabolism in the order of decreasing efficacy: SP > EP > GLC, and (4) all fuels restored the amount of glutamate and glutamine labeled via PC compared to SAL-treated animals suggesting improvements in astrocyte metabolism.

4.1. Physiological effects of CCI and SAL, SP, EP or GLC treatments

Prior to the infusion of ^{13}C glucose, the arterial pH and HCO_3 measures taken 1 h after the final SAL or fuel treatment were higher in the CCI-SP group compared to all other groups and remained higher in the SP group at 15 and 67 min into the ^{13}C glucose infusion compared to the other groups. These findings are consistent with previous reports of elevated pH and HCO_3 levels following systemic administration of SP (Fukushima et al., 2009; Mongan et al., 2001).

The plasma glucose concentrations pre- and post-infusion of [1,2 $^{13}C_2$] glucose and the ^{13}C enrichment of plasma glucose did not differ between groups, indicating that differences in brain metabolite labeling were not due to differences in substrate infusion. However, it should be noted that the pre-infusion plasma lactate concentration was elevated in the CCI-GLC group when compared to CCI-SAL and remained elevated at 15 min after beginning the ^{13}C glucose infusion when compared to the CCI-SAL and CCI-EP groups. Higher pre-infusion plasma lactate concentrations may have confounded the ^{13}C tissue findings in the CCI-GLC group as the utilization of lactate has been reported in the injured brain (Glenn et al., 2015). This could result in substrate (^{13}C) dilution lowering the amount of recovered ^{13}C labeled tissue metabolites, leading to an underestimation of the effect of GLC on neuronal and astrocyte oxidative metabolism.

4.2. Glucose utilization, glycolysis and TCA cycle

In all CCI groups, the total ^{13}C glucose pool in the left hemisphere was significantly increased compared to the Sham group. This finding differs from our previous finding after a 3 h infusion of [1,2 $^{13}C_2$] glucose in this CCI injury model (Bartnik et al., 2005), but is similar to our observation of a pool of unmetabolized [1,2 $^{13}C_2$] glucose in cortex at 24 h after a fluid percussion brain injury (Bartnik et al., 2007). The increase in ^{13}C labeled glucose in the injured tissue may reflect decreased metabolism as supported by the concomitant reduction in oxidative metabolism in all CCI groups (Fig. 2). However, there was a substantial, albeit non-significant, increase in the ^{13}C glucose pool size with fuel treatments versus CCI-SAL that may reflect a higher brain glucose uptake in the SP, EP and GLC groups. In studies using [^{14}C]2-deoxy-D-glucose autoradiography, these same doses of pyruvate and glucose were shown to attenuate reductions in cerebral glucose utilization at 24 h post-injury (Moro et al., 2013, 2016). Moreover, the metabolism of supplemental exogenous SP, EP or GLC may have a “glucose sparing” effect, as prior research has shown that systemic administration of either lactate (Chen et al., 2000) or SP (Fukushima et al., 2009) attenuated a TBI-induced reduction of extracellular glucose levels.

Compared to Sham-injured control animals, CCI-SAL animals (osmolarity controls) showed moderate but non-significant increases in ^{13}C lactate labeled via glycolysis and significantly reduced amounts of ^{13}C glutamate and glutamine labeled in the first turn of the TCA cycle in the injured tissue 24 h. This indicates increased glycolysis and reduced neuronal oxidative metabolism. Since the period of increased energy demand for elevated glycolysis is generally short (minutes to hours) in experimental TBI (Katayama et al., 1990; Lee et al., 1999; Sutton et al., 1994; Yoshino et al., 1991), the accumulation of labeled lactate at 24 h post-CCI may be due to impaired PDH activity or respiration in mitochondria (Opii et al.,

2007; Xing et al., 2009; Xiong et al., 1997). Schuhmann et al. (2003). have reported increased lactate levels at 24 h post-CCI in regions exhibiting increased activity of glutamate dehydrogenase, an enzyme metabolizing glutamate that is preferentially localized within astrocytes. Enhanced glutamate dehydrogenase activity could suggest an increase in the astrocyte uptake of glutamate following injury. In cultured rat brain astrocytes, exogenous glutamate taken up from the culture medium is oxidized primarily by astrocytes via glutamate dehydrogenase and partial pyruvate recycling with lactate as a byproduct (McKenna, 2013).

Lastly, potential osmotic effects of our treatments may have contributed to the increase in lactate labeled via glycolysis ([2,3 $^{13}C_2$] lactate) observed in CCI-injured groups. Elevated blood cation levels in the presence of blood brain barrier (BBB) damage may enhance spreading depression leading to an increase in glycolysis. All treatments were injected intraperitoneally (i.p.) with the final treatment 1 h preceding [1,2 $^{13}C_2$] glucose infusion to reduce the potential osmotic effects. However, it has been reported that a 4 ml/kg bolus of hypertonic saline (7.5%) increases plasma osmolarity up to 4 h after intravenous administration (Elliott et al., 2009). It is possible that osmotic effects contributed to our findings, as the amount of ^{13}C lactate in the SAL treated group, which had the lowest calculated osmolarity, was significantly lower than the ^{13}C lactate in the SP, EP and GLC treatment groups. Future studies assessing brain tissue and plasma osmolarity in conjunction with the metabolic effects of i.p. administration of these biofuels appear warranted.

The decrease in the total amount of ^{13}C labeled glutamate in the CCI-SAL group was the result of decreased ^{13}C glutamate labeling via both PDH and PC, which is also consistent with the previous reports of impaired PDH activity (Opii et al., 2007; Xing et al., 2009; Xiong et al., 1997). The reduced ^{13}C glutamate labeling via PC, an astrocyte-specific enzyme, could suggest a decrease in the trafficking of glutamine to the neuronal compartment via the glutamate-glutamine cycle. While we did not directly measure glutamate-glutamine cycling, reduced glutamine isotopomer labeling in the CCI-SAL group supports this idea. In a previous study using this approach, we found that the total amount of ^{13}C glutamate and ^{13}C glutamine in the injured cortex were reduced at 24 h post-CCI, but they did not reach statistical significance compared to Shams (Bartnik et al., 2005). The discrepancy between the two studies may be the result of differences in tissue sampling (cortex vs. cortex + underlying hippocampus), infusion duration (3 h versus 68 min), and tissue extraction methods (perchloric acid versus methanol and chloroform).

Following fuel treatment, the injured tissue of CCI injured animals treated with SP, EP and GLC also showed significantly increased amounts of ^{13}C lactate labeled by the PPP + PR pathway and glycolysis compared to Sham levels, suggesting that all three fuels enhanced glycolysis. Increased amounts of tissue ^{13}C lactate following pyruvate treatment is compatible with reports that pyruvate, in its conversion to lactate via reversible pyruvate carboxylation and partial pyruvate recycling (Gonzalez et al., 2005), can counteract reductions in NAD^+ and restore the NAD^+/NADH redox state necessary to counteract glycolytic inhibition in neuronal injury models (Mongan et al., 2003; Sheline et al., 2000; Zeng et al., 2007).

Although the total amount of ^{13}C glutamate was reduced in the injured tissue of SP, EP and GLC treatment groups compared to the Shams, the ^{13}C glutamate pool was highest in the CCI-SP group. This suggests SP improved neuronal oxidative metabolism, compared to all other fuels, which is supported by findings of similar amounts of PDH-derived glutamate as Shams. Likewise, SP was the only fuel treatment to restore the total amount of ^{13}C glutamine as well as the amount of PDH-derived glutamine. These beneficial effects of SP treatments may be related to ability of pyruvate to alter PDH activity or levels in the brain (Mongan et al., 2003; Sharma et al., 2009). The CCI-SP group also had similar amounts of PC-derived glutamate and glutamine as the Sham group, indicating improved astrocyte metabolism following SP treatment.

Although EP treatment did not improve neuronal oxidative metabolism, as measured by the restoration of glutamate labeling, the amount of ^{13}C glutamate and ^{13}C glutamine labeling via PC were restored to Sham levels suggesting that EP enhanced astrocyte metabolism by ameliorating the injury-induced decrease in astrocyte PC activity. Similarly CCI-injured animals treated with GLC group showed reduced ^{13}C glutamate synthesized via PDH and PC, compared to Sham controls, consistent with reduced neuronal metabolism. However, the amount of ^{13}C glutamine derived from both PDH and PC were not different from Sham, suggesting that GLC only partially restored the injury-induced decrease in astrocyte PDH and PC activity. The mismatch between glutamate and glutamine labeling after GLC treatment suggests that the exchange of metabolites via glutamate-glutamine cycling was altered in this group. The restoration of ^{13}C glutamine synthesis via PC following SP, EP and GLC treatments reflects the ability of these post-TBI treatments to restore anaplerotic function and potentially replace carbons lost to glutamine efflux in support of neurotransmitter trafficking. The overall reduction in the amount of ^{13}C glutamate measured in the CCI-SP and CCI-EP groups are somewhat contrary to a previous study where i.p. pyruvate injections along a similar time course attenuated CCI-induced reductions in cytochrome oxidase activity at 72 h post-injury, indicating general cellular neuroprotection (Moro and Sutton, 2010). However, it is likely that the enduring reduction in glutamate ^{13}C-labeling reflects a specific loss of glutamatergic neurons, as the neuroprotective properties of SP, EP and GLC are incomplete in TBI models (Fukushima et al., 2009; Moro et al., 2013, 2016; Moro and Sutton, 2010; Shijo et al., 2015; Zlotnik et al., 2008, 2012).

4.3. The pentose phosphate pathway and pyruvate recycling

In addition to glycolysis, lactate can be labeled from the metabolism of [1,2 $^{13}C_2$] glucose via the PPP and/or from the decarboxylation of oxaloacetate or malate via partial pyruvate recycling. In both instances, lactate will be labeled in the [3 ^{13}C] singlet position, making it impossible to differentiate the contribution of the PPP + PR pathway to the labeling of ^{13}C lactate. In this study we used the ratio of [3 ^{13}C] lactate to [2,3 $^{13}C_2$] lactate to estimate the relative contribution of the PPP + PR pathway to lactate labeling, in an attempt to identify injury or fuel specific shifts in these metabolic pathways. In the CCI-SAL group, the contribution of PPP + PR pathway, relative to glycolysis was ~17% (Table 3) which was significantly higher than the Sham group (Table 3). This finding suggests an injury induced increase in the PPP and PR pathway. While we cannot differentiate between the contributions of these two pathways, an injury-induced increase in the metabolism of

glucose via the PPP could reflect a need for increased reducing equivalents in the form of NADPH (Baquer et al., 1988; Hothersall et al., 1982; Schrader et al., 1993), whereas an injury-induced increase in pyruvate recycling could reflect increased decarboxylation of glutamate as a method of increasing cellular ATP levels (McKenna, 2013). We previously reported an increase in glucose metabolism via the PPP following experimental TBI (Bartnik et al., 2005, 2007) and our current finding is consistent with those observations. With fuel treatment, there was an increase in lactate labeling by both the PPP + PR pathway and glycolysis (Table 2), suggesting that more glucose was available for metabolism in these animals.

The relative contribution of the PPP + PR pathway to glutamate labeling in SAL, EP and GLC treated animals was similar to Shams, which was due to a reduction in the relative amounts of [4 ^{13}C] and [4,5 $^{13}C_2$] glutamate. In contrast, an increase in the contribution of the PPP + PR pathway was seen in the CCI-SP group, driven by a trend towards an increase in the relative amount of [4 ^{13}C] glutamate, suggesting an increase in the oxidation of [3 ^{13}C] lactate derived from either pathway via PDH. Since the amount of [4,5 $^{13}C_2$] glutamate labeling via PDH was also increased in this group, it would indicate that SP treatment improves neuronal oxidative metabolism.

In the contralateral hemisphere, the CCI-SAL group showed a significant increase in the total ^{13}C glucose and in the total ^{13}C lactate pool as well as lactate derived from glycolysis compared to the Sham group. This is consistent with enhanced involvement of this region with ipsilateral function and connectivity (Harris et al., 2013, 2016). In addition, the CCI-SAL group showed reduced ^{13}C glutamine synthesis via PC and a reduction of the PC/PDH ratio for glutamine suggesting reduced anaplerotic activity following injury. These findings indicate adaptations to glucose metabolism, glycolysis, and astrocyte metabolism that suggest the presence of milder injury to the contralateral hemisphere following unilateral CCI. Similar effects were found in GLC-treated, but not in SP or EP groups, suggesting the pyruvate compounds ameliorated some of these milder injury effects in the contralateral hemisphere.

In summary, the widely varied doses of SP, EP and GLC examined in this study all enhanced lactate labeling but differentially affected neuronal or astrocyte metabolism after CCI injury. This study was not designed to be an equimolar comparison between fuels, but rather an examination of each fuel's effect on glucose metabolism using previously reported neuroprotective doses. The restoration of astrocyte metabolism by all three fuels may partially contribute to their ability to improve cerebral glucose utilization and to reduce cortical and hippocampal neuronal loss at 24 h post-CCI (Moro et al., 2013, 2016).

Supplementary Material

Refer to Web version on PubMed Central for supplementary material.

Acknowledgments

This work was supported by the UCLA Brain Injury Research Center and award PO1NS058489 from the National Institute of Neurological Disorders and Stroke (NINDS). The content is the sole responsibility of the authors and does not necessarily represent official views of the NINDS or the National Institutes of Health.

Abbreviations

CCI	controlled cortical impact
EP	ethyl pyruvate
GABA	γ amino butyric acid
GAPDH	glyceraldehyde-3-phosphate dehydrogenase
GLC	glucose
HCO_3	bicarbonate
LDH	lactate dehydrogenase
ME	malic enzyme
NAD^+/NADH	oxidized/reduced form of nicotinamide adenine dinucleotide
NADPH	nicotinamide adenine dinucleotide phosphate
NMR	nuclear magnetic resonance spectroscopy
O_2 Sat	oxygen saturation
PARP	poly (ADP-ribose) polymerases
PC	pyruvate carboxylase
pCO_2	partial pressure of carbon dioxide
PDH	pyruvate dehydrogenase
PEPCK	phosphoenolpyruvate carboxykinase
PK	pyruvate kinase
pO_2	partial pressure of oxygen
PPP	pentose phosphate pathway
PR	pyruvate recycling
SAL	saline
SP	sodium pyruvate
TBI	traumatic brain injury
TCA	tricarboxylic acid

TSP sodium-(trimethylsilyl) propionate

References

Alessandri B, Doppenberg E, Zauner A, Woodward J, Choi S, Bullock R. Evidence for time-dependent glutamate-mediated glycolysis in head-injured patients: a microdialysis study. Acta Neurochir Suppl. 1999; 75:25–28. [PubMed: 10635372]

Andrabi SA, Umanah GK, Chang C, Stevens DA, Karuppagounder SS, Gagne JP, Poirier GG, Dawson VL, Dawson TM. Poly(ADP-ribose) polymerase-dependent energy depletion occurs through inhibition of glycolysis. Proc Natl Acad Sci U S A. 2014; 111:10209–10214. [PubMed: 24987120]

Badar-Goffer RS, Bachelard HS, Morris PG. Cerebral metabolism of acetate and glucose studied by 13C-n.m.r. spectroscopy. A technique for investigating metabolic compartmentation in the brain. Biochem J. 1990; 266:133–139. [PubMed: 1968742]

Baquer NZ, Hothersall JS, McLean P. Function and regulation of the pentose phosphate pathway in brain. Curr Top Cell Regul. 1988; 29:265–289. [PubMed: 3293926]

Bartnik BL, Lee SM, Hovda DA, Sutton RL. The fate of glucose during the period of decreased metabolism after fluid percussion injury: a 13C NMR study. J Neurotrauma. 2007; 24:1079–1092. [PubMed: 17610349]

Bartnik BL, Sutton RL, Fukushima M, Harris NG, Hovda DA, Lee SM. Upregulation of pentose phosphate pathway and preservation of tricarboxylic acid cycle flux after experimental brain injury. J Neurotrauma. 2005; 22:1052–1065. [PubMed: 16238483]

Bartnik-Olson BL, Oyoyo U, Hovda D, Sutton RL. Astrocyte oxidative metabolism and metabolite trafficking after fluid percussion brain injury in adult rats. J Neurotrauma. 2010; 27:2191–2202. [PubMed: 20939699]

Bergsneider M, Hovda DA, Lee SM, Kelly DF, McArthur DL, Vespa PM, Lee JH, Huang SC, Martin NA, Phelps ME, Becker DP. Dissociation of cerebral glucose metabolism and level of consciousness during the period of metabolic depression following human traumatic brain injury. J Neurotrauma. 2000; 17:389–401. [PubMed: 10833058]

Besson VC, Croci N, Boulu RG, Plotkine M, Marchand-Verrecchia C. Deleterious poly(ADP-ribose)polymerase-1 pathway activation in traumatic brain injury in rat. Brain Res. 2003; 989:58–66. [PubMed: 14519512]

Bligh EG, Dyer WJ. A rapid method of total lipid extraction and purification. Can J Biochem Physiol. 1959; 37:911–917. [PubMed: 13671378]

Chen S, Pickard JD, Harris NG. Time course of cellular pathology after controlled cortical impact injury. Exp Neurol. 2003; 182:87–102. [PubMed: 12821379]

Chen T, Qian YZ, Di X, Rice A, Zhu JP, Bullock R. Lactate/glucose dynamics after rat fluid percussion brain injury. J Neurotrauma. 2000; 17:135–142. [PubMed: 10709871]

Clark RS, Vagni VA, Nathaniel PD, Jenkins LW, Dixon CE, Szabo C. Local administration of the poly(ADP-ribose) polymerase inhibitor INO-1001 prevents NAD+ depletion and improves water maze performance after traumatic brain injury in mice. J Neurotrauma. 2007; 24:1399–1405. [PubMed: 17711401]

Cruz F, Cerdan S. Quantitative 13C NMR studies of metabolic compartmentation in the adult mammalian brain. NMR Biomed. 1999; 12:451–462. [PubMed: 10654292]

Dhillon HS, Dose JM, Scheff SW, Prasad MR. Time course of changes in lactate and free fatty acids after experimental brain injury and relationship to morphologic damage. Exp Neurol. 1997; 146:240–249. [PubMed: 9225757]

Dunn-Meynell AA, Levin BE. Histological markers of neuronal, axonal and astrocytic changes after lateral rigid impact traumatic brain injury. Brain Res. 1997; 761:25–41. [PubMed: 9247063]

Elliott MB, Jallo JJ, Barbe MF, Tuma RF. Hypertonic saline attenuates tissue loss and astrocyte hypertrophy in a model of traumatic brain injury. Brain Res. 2009; 1305:183–191. [PubMed: 19804766]

Fukushima M, Lee SM, Moro N, Hovda DA, Sutton RL. Metabolic and histologic effects of sodium pyruvate treatment in the rat after cortical contusion injury. J Neurotrauma. 2009; 26:1095–1110. [PubMed: 19594384]

Glenn TC, Martin NA, Horning MA, McArthur DL, Hovda D, Vespa PM, Brooks GA. Lactate: brain fuel in human traumatic brain injury. A comparison to normal healthy control subjects. J Neurotrauma. 2015; 32:820–832. [PubMed: 25594628]

Gonzalez SV, Nguyen NH, Rise F, Hassel B. Brain metabolism of exogenous pyruvate. J Neurochem. 2005; 95:284–293. [PubMed: 16181432]

Govindaraju V, Young K, Maudsley AA. Proton NMR chemical shifts and coupling constants for brain metabolites. NMR Biomed. 2000; 13:129–153. [PubMed: 10861994]

Hall ED, Andrus PK, Yonkers PA. Brain hydroxyl radical generation in acute experimental head injury. J Neurochem. 1993; 60:588–594. [PubMed: 8380437]

Hall ED, Detloff MR, Johnson K, Kupina NC. Peroxynitrite-mediated protein nitration and lipid peroxidation in a mouse model of traumatic brain injury. J Neurotrauma. 2004; 21:9–20. [PubMed: 14987461]

Harris NG, Plant HD, Briggs RW, Jones HC. Metabolite changes in the cerebral cortex of treated and untreated infant hydrocephalic rats studied using in vitro 31P-NMR spectroscopy. J Neurochem. 1996; 67:2030–2038. [PubMed: 8863510]

Harris NG, Chen SF, Pickard JD. Cortical reorganization after experimental traumatic brain injury: a functional autoradiography study. J Neurotrauma. 2013; 30(13):1137–1146. [PubMed: 23305562]

Harris NG, Verley DR, Gutman BA, Thompson PM, Yeh HJ, Brown JA. Disconnection and hyper-connectivity underlie reorganization after TBI: a rodent functional connectomic analysis. Exp Neurol. 2016; 277:124–138. [PubMed: 26730520]

Hellmich HL, Eidson KA, Capra BA, Garcia JM, Boone DR, Hawkins BE, Uchida T, Dewitt DS, Prough DS. Injured Fluoro-Jade-positive hippocampal neurons contain high levels of zinc after traumatic brain injury. Brain Res. 2007; 1127:119–126. [PubMed: 17109824]

Hothersall JS, Greenbaum AL, McLean P. The functional significance of the pentose phosphate pathway in synaptosomes: protection against peroxidative damage by catecholamines and oxidants. J Neurochem. 1982; 39:1325–1332. [PubMed: 7119799]

Hovda DA, Yoshino A, Kawamata T, Katayama Y, Becker DP. Diffuse prolonged depression of cerebral oxidative metabolism following concussive brain injury in the rat: a cytochrome oxidase histochemistry study. Brain Res. 1991; 567:1–10. [PubMed: 1667742]

Humphries KM, Szweda LI. Selective inactivation of alpha-ketoglutarate dehydrogenase and pyruvate dehydrogenase: reaction of lipoic acid with 4-hydroxy-2-nonenal. Biochemistry. 1998; 37:15835–15841. [PubMed: 9843389]

Katayama Y, Becker DP, Tamura T, Hovda DA. Massive increases in extracellular potassium and the indiscriminate release of glutamate following concussive brain injury. J Neurosurg. 1990; 73:889–900. [PubMed: 1977896]

Katayama Y, Maeda T, Koshinaga M, Kawamata T, Tsubokawa T. Role of excitatory amino acid-mediated ionic fluxes in traumatic brain injury. Brain Pathol. 1995; 5:427–435. [PubMed: 8974625]

Kawamata T, Katayama Y, Hovda DA, Yoshino A, Becker DP. Administration of excitatory amino acid antagonists via microdialysis attenuates the increase in glucose utilization seen following concussive brain injury. J Cereb Blood Flow Metab. 1992; 12:12–24. [PubMed: 1345756]

Kawamata T, Katayama Y, Hovda DA, Yoshino A, Becker DP. Lactate accumulation following concussive brain injury: the role of ionic fluxs induced by excitatory amino acids. Brain Res. 1995; 674:196–204. [PubMed: 7540925]

Kochanek AR, Kline AE, Gao WM, Chadha M, Lai Y, Clark RS, Dixon CE, Jenkins LW. Gel-based hippocampal proteomic analysis 2 weeks following traumatic brain injury to immature rats using controlled cortical impact. Dev Neurosci. 2006; 28:410–419. [PubMed: 16943664]

Krishnappa IK, Contant CF, Robertson CS. Regional changes in cerebral extracellular glucose and lactate concentrations following severe cortical impact injury and secondary ischemia in rats. J Neurotrauma. 1999; 16:213–224. [PubMed: 10195469]

Laplaca MC, Raghupathi R, Verma A, Pieper AA, Saatman KE, Snyder SH, McIntosh TK. Temporal patterns of poly(ADP-ribose) polymerase activation in the cortex following experimental brain injury in the rat. J Neurochem. 1999; 73:205–213. [PubMed: 10386972]

Le Belle JE, Harris NG, Williams SR, Bhakoo KK. A comparison of cell and tissue extraction techniques using high-resolution 1H-NMR spectroscopy. NMR Biomed. 2002; 15:37–44. [PubMed: 11840551]

Lee SM, Wong DA, Samii A, Hovda DA. Evidence for energy failure following irreversible traumatic brain injury. Ann N Y Acad Sci. 1999; 893:337–340. [PubMed: 10672261]

Marklund N, Clausen F, Ander TL, Hillered L. Monitoring of reactive oxygen species production after traumatic brain injury in rats with microdialysis and the 4-hydroxybenzoic acid trapping method. J Neurotrauma. 2001; 18:1217–1227. [PubMed: 11721740]

Marklund N, Salci K, Ronquist G, Hillered L. Energy metabolic changes in the early post-injury period following traumatic brain injury in rats. Neurochem Res. 2006; 31:1085–1093. [PubMed: 16909313]

McKenna M. Glutmate pays its own way in astrocytes. Front Endocrinol. 2013; 4:1–6. Article 191.

Miccheli A, Aureli T, Delfini M, Di Cocco ME, Viola P, Gobetto R, Conti F. Study on influence of inactivation enzyme techniques and extraction procedures on cerebral phosphorylated metabolite levels by 31P NMR spectroscopy. Cell Mol Biol. 1988; 34:591–603. [PubMed: 3219695]

Mongan PD, Capacchione J, Fontana JL, West S, Bunger R. Pyruvate improves cerebral metabolism during hemorrhagic shock. Am J Physiol Heart Circ Physiol. 2001; 281:H854–H864. [PubMed: 11454591]

Mongan PD, Karaian J, Van Der Schuur BM, Via DK, Sharma P. Pyruvate prevents poly-ADP ribose polymerase (PARP) activation, oxidative damage, and pyruvate dehydrogenase deactivation during hemorrhagic shock in swine. J Surg Res. 2003; 112:180–188. [PubMed: 12888336]

Morken TS, Brekke E, Haberg A, Wideroe M, Brubakk AM, Sonnewald U. Neuron-astrocyte interactions, pyruvate carboxylation and the pentose phosphate pathway in the neonatal rat brain. Neurochem Res. 2014; 39:556–569. [PubMed: 23504293]

Moro N, Ghavim S, Harris NG, Hovda DA, Sutton RL. Glucose administration after traumatic brain injury improves cerebral metabolism and reduces secondary neuronal injury. Brain Res. 2013; 1535:124–136. [PubMed: 23994447]

Moro N, Ghavim SS, Harris NG, Hovda DA, Sutton RL. Pyruvate treatment attenuates cerebral metabolic depression and neuronal loss after experimental traumatic brain injury. Brain Res. 2016; 1642:270–277. [PubMed: 27059390]

Moro N, Sutton RL. Beneficial effects of sodium or ethyl pyruvate after traumatic brain injury in the rat. Exp Neurol. 2010; 225:391–401. [PubMed: 20670624]

Nilsson P, Hillered L, Ponten U, Ungerstedt U. Changes in cortical extra-cellular levels of energy-related metabolites and amino acids following concussive brain injury in rats. J Cereb Blood Flow Metab. 1990; 10:631–637. [PubMed: 2384536]

Opii WO, Nukala VN, Sultana R, Pandya JD, Day KM, Merchant ML, Klein JB, Sullivan PG, Butterfield DA. Proteomic identification of oxidized mitochondrial proteins following experimental traumatic brain injury. J Neurotrauma. 2007; 24:772–789. [PubMed: 17518533]

Palmer AM, Marion DW, Botscheller ML, Swedlow PE, Styren SD, Dekosky ST. Traumatic brain injury-induced excitotoxicity assessed in a controlled cortical impact model. J Neurochem. 1993; 61:2015–2024. [PubMed: 7504079]

Prins ML, Hovda DA. The effects of age and ketogenic diet on local cerebral metabolic rates of glucose after controlled cortical impact injury in rats. J Neurotrauma. 2009; 26:1083–1093. [PubMed: 19226210]

Ralser M, Wamelink MM, Kowald A, Gerisch B, Heeren G, Struys EA, Klipp E, Jakobs C, Breitenbach M, Lehrach H, Krobitsch S. Dynamic rerouting of the carbohydrate flux is key to counteracting oxidative stress. J Biol. 2007; 6:10. [PubMed: 18154684]

Rose ME, Huerbin MB, Melick J, Marion DW, Palmer AM, Schiding JK, Kochanek PM, Graham SH. Regulation of interstitial excitatory amino acid concentrations after cortical contusion injury. Brain Res. 2002; 935:40–46. [PubMed: 12062471]

Satchell MA, Zhang X, Kochanek PM, Dixon CE, Jenkins LW, Melick J, Szabo C, Clark RS. A dual role for poly-ADP-ribosylation in spatial memory acquisition after traumatic brain injury in mice involving NAD+ depletion and ribosylation of 14-3-3gamma. J Neurochem. 2003; 85:697–708. [PubMed: 12694396]

Schrader MC, Eskey CJ, Simplaceanu V, Ho C. A carbon-13 nuclear magnetic resonance investigation of the metabolic fluxes associated with glucose metabolism in human erythrocytes. Biochim Biophys Acta. 1993; 1182:162–178. [PubMed: 8357848]

Schuhmann MU, Stiller D, Skardelly M, Bernarding J, Klinge PM, Samii A, Samii M, Brinker T. Metabolic changes in the vicinity of brain contusions: a proton magnetic resonance spectroscopy and histology study. J Neurotrauma. 2003; 20:725–743. [PubMed: 12965052]

Sharma P, Benford B, Li ZZ, Ling GS. Role of pyruvate dehydrogenase complex in traumatic brain injury and measurement of pyruvate dehydrogenase enzyme by dipstick test. J Emerg Trauma Shock. 2009; 2:67–72. [PubMed: 19561963]

Sheline CT, Behrens MM, Choi DW. Zinc-induced cortical neuronal death: contribution of energy failure attributable to loss of NAD(+) and inhibition of glycolysis. J Neurosci. 2000; 20:3139–3146. [PubMed: 10777777]

Shijo K, Ghavim S, Harris NG, Hovda DA, Sutton RL. Glucose administration after traumatic brain injury exerts some benefits and no adverse effects on behavioral and histological outcomes. Brain Res. 2015; 1614:94–104. [PubMed: 25911580]

Schousboe, A. A tribute to Mary C. McKenna: glutamate as energy substrate and neurotransmitter - functional interaction between neurons and astrocytes. Neurochem Res. 2015. http://dx.doi.org/10.1007/s11064-015-1813-9

Sonnewald U, Rae C. Pyruvate carboxylation in different model systems studied by (13)C MRS. Neurochem Res. 2010; 35:1916–1921. [PubMed: 20842423]

Sugimori H, Ibayashi S, Fujii K, Nagao T, Sadoshima S, Fujishima M. Mild hyperglycemia and insulin treatment in experimental cerebral ischemia in rats. Brain Res Bull. 1996; 40(4):263–268. [PubMed: 8842410]

Suh SW, Chen JW, Motamedi M, Bell B, Listiak K, Pons NF, Danscher G, Frederickson CJ. Evidence that synaptically-released zinc contributes to neuronal injury after traumatic brain injury. Brain Res. 2000; 852:268–273. [PubMed: 10678752]

Suh SW, Frederickson CJ, Danscher G. Neurotoxic zinc translocation into hippocampal neurons is inhibited by hypothermia and is aggravated by hyperthermia after traumatic brain injury in rats. J Cereb Blood Flow Metab. 2006; 26:161–169. [PubMed: 15988476]

Sunami K, Nakamura T, Ozawa Y, Kubota M, Namba H, Yamaura A. Hypermetabolic state following experimental head injury. Neurosurg Rev. 1989; 12(Suppl 1):400–411. [PubMed: 2812406]

Sutton, RL.; Hovda, DA.; Adelson, PD.; Benzel, EC.; Becker, DP. Acta Neurochir. Vol. 60. Wien: 1994. Metabolic changes following cortical contusion: relationships to edema and morphological changes; p. 446-448.

Sutton RL, Lescaudron L, Stein DG. Unilateral cortical contusion injury in the rat: vascular disruption and temporal development of cortical necrosis. J Neurotrauma. 1993; 10:135–149. [PubMed: 8411217]

Tabatabaie T, Potts JD, Floyd RA. Reactive oxygen species-mediated inactivation of pyruvate dehydrogenase. Arch Biochem Biophys. 1996; 336:290–296. [PubMed: 8954577]

Tavazzi B, Signoretti S, Lazzarino G, Amorini AM, Delfini R, Cimatti M, Marmarou A, Vagnozzi R. Cerebral oxidative stress and depression of energy metabolism correlate with severity of diffuse brain injury in rats. Neurosurgery. 2005; 56:582–589. [PubMed: 15730584]

Verweij BH, Muizelaar JP, Vinas FC, Peterson PL, Xiong Y, Lee CP. Mitochondrial dysfunction after experimental and human brain injury and its possible reversal with a selective N-type calcium channel antagonist (SNX-111). Neurol Res. 1997; 19:337–339.

Xing G, Ren M, O'Neill JT, Sharma P, Verma A, Watson WD. Pyruvate dehydrogenase phosphatase1 mRNA expression is divergently and dynamically regulated between rat cerebral cortex, hippocampus and thalamus after traumatic brain injury: a potential biomarker of TBI-induced hyper- and hypoglycaemia and neuronal vulnerability. Neurosci Lett. 2012; 525:140–145. [PubMed: 22884618]

Xing G, Ren M, Watson WA, O'Neil JT, Verma A. Traumatic brain injury-induced expression and phosphorylation of pyruvate dehydrogenase: a mechanism of dysregulated glucose metabolism. Neurosci Lett. 2009; 454:38–42. [PubMed: 19429050]

Xiong Y, Gu Q, Peterson PL, Muizelaar JP, Lee CP. Mitochondrial dysfunction and calcium perturbation induced by traumatic brain injury. J Neurotrauma. 1997; 14:23–34. [PubMed: 9048308]

Yoshino A, Hovda DA, Kawamata T, Katayama Y, Becker DP. Dynamic changes in local cerebral glucose utilization following cerebral concussion in rats: evidence of a hyper- and subsequent hypometabolic state. Brain Res. 1991; 561:106–119. [PubMed: 1797338]

Zeng J, Yang GY, Ying W, Kelly M, Hirai K, James TL, Swanson RA, Litt L. Pyruvate improves recovery after PARP-1-associated energy failure induced by oxidative stress in neonatal rat cerebrocortical slices. J Cereb Blood Flow Metab. 2007; 27:304–315. [PubMed: 16736046]

Zlotnik A, Gurevich B, Cherniavsky E, Tkachov S, Matuzani-Ruban A, Leon A, Shapira Y, Teichberg VI. The contribution of the blood glutamate scavenging activity of pyruvate to its neuroprotective properties in a rat model of closed head injury. Neurochem Res. 2008; 33:1044–1050. [PubMed: 18080187]

Zlotnik A, Sinelnikov I, Gruenbaum BF, Gruenbaum SE, Dubilet M, Dubilet E, Leibowitz A, Ohayon S, Regev A, Boyko M, Shapira Y, Teichberg VI. Effect of glutamate and blood glutamate scavengers oxaloacetate and pyruvate on neurological outcome and pathohistology of the hippocampus after traumatic brain injury in rats. Anesthesiology. 2012; 116:73–83. [PubMed: 22129535]

Appendix A. Supplementary data

Supplementary data related to this article can be found at http://dx.doi.org/10.1016/j.neuint.2016.11.014.

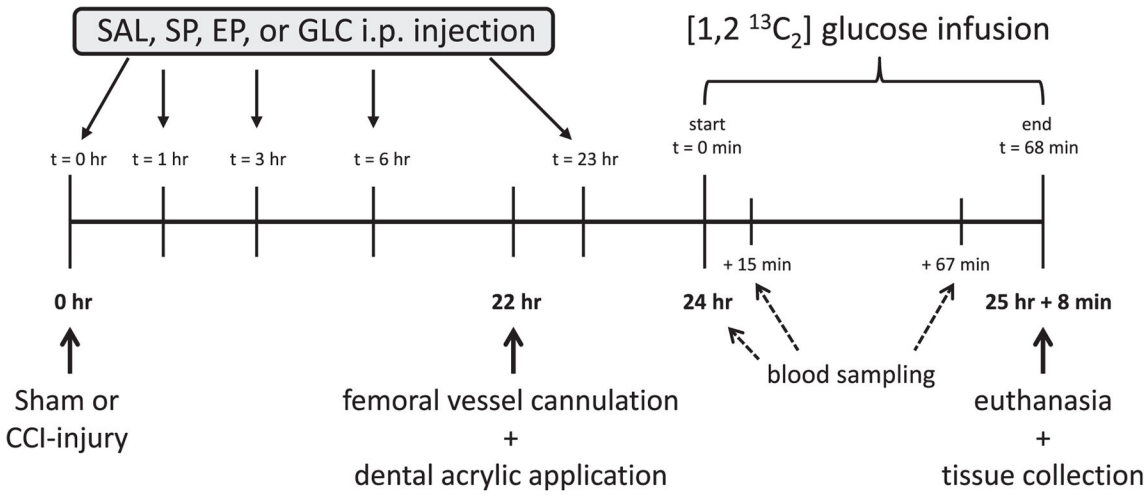

Fig. 1.

Timeline of post-surgical experimental procedures. Intraperitoneal injections of SAL, SP, EP or GLC were administered at 0, 1, 3, 6 and 23 h post-CCI injury. [1,2 $^{13}C_2$] labeled glucose was infused for 68 min starting at 24 h after CCI-injury. Arterial blood samples were taken prior to and at 15 and 67 min after the infusion of [1,2 $^{13}C_2$] glucose. CCI, controlled cortical impact; EP, ethyl pyruvate; GLC, glucose; SAL, saline; SP, sodium pyruvate.

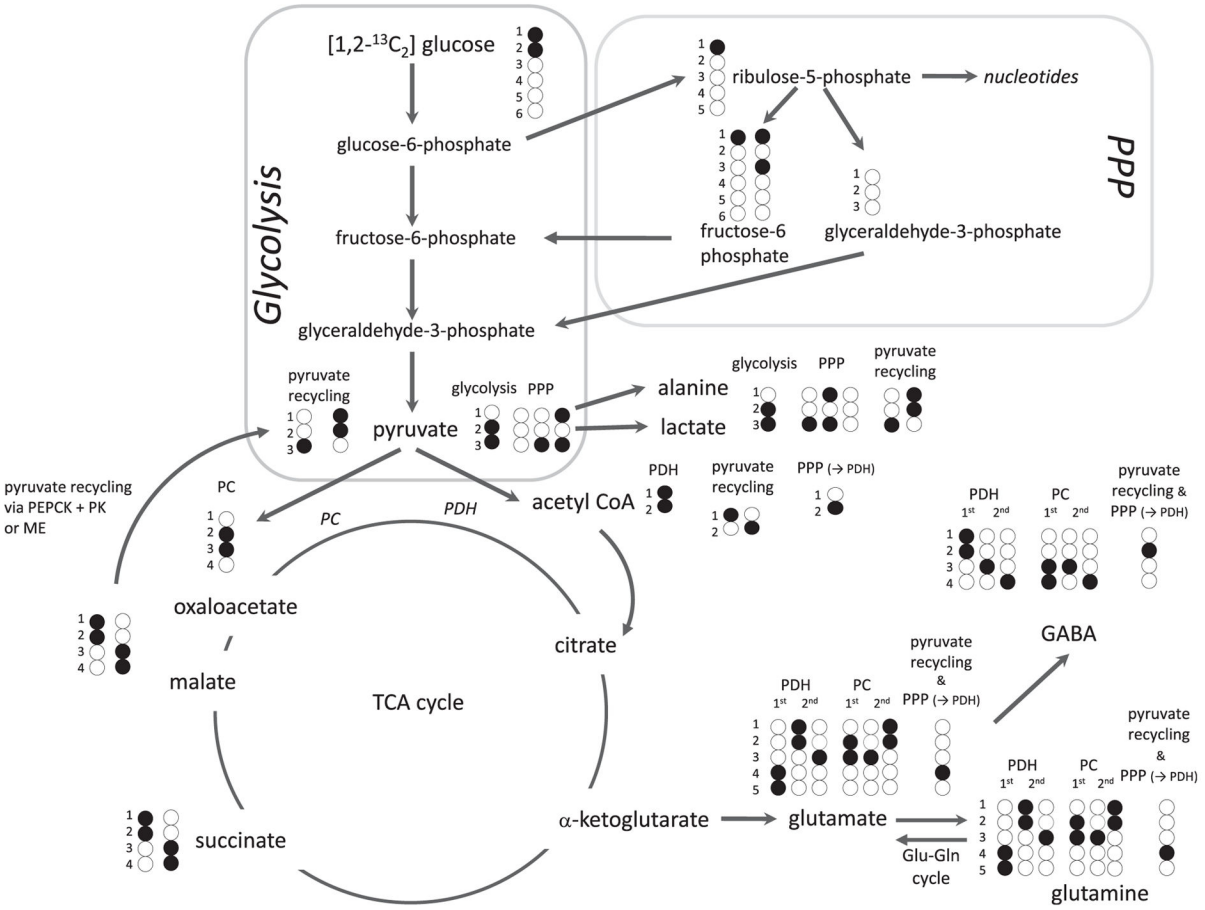

Fig. 2.

^{13}C labeling scheme following an infusion of [1,2 $^{13}C_2$] glucose. Black circles denote the possible position of ^{13}C labeling on carbon backbones during metabolism. The isotopomers resulting from metabolism through glycolysis, the oxidative branch of the PPP, the first and second turns of the TCA cycle, and pyruvate recycling are shown. Gln, glutamine; Glu, glutamate; ME, malic enzyme; PC, pyruvate carboxylase; PDH, pyruvate dehydrogenase; PEPCK, phosphoenolpyruvate carboxykinase; PK, pyruvate kinase; PPP, pentose phosphate pathway; TCA, tricarboxylic acid cycle.

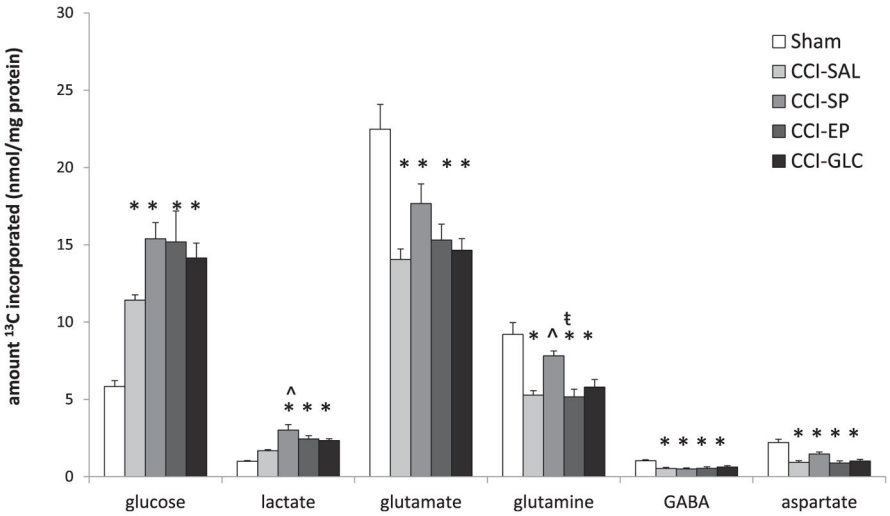

Fig. 3.

The total amount (nmol/mg protein) of ^{13}C labeled glucose, lactate, glutamate, glutamine, GABA, and aspartate metabolite pools of the left (injured) cortex + hippocampus samples. CCI, controlled cortical impact; EP, ethyl pyruvate; GLC, glucose; SAL, saline; SP, sodium pyruvate. All values are expressed as mean ± SEM. *$p < 0.05$ versus Sham; ^ $p < 0.05$ versus CCI-SAL; ŧ $p < 0.05$ versus CCI-SP using one-way ANOVA with Bonferroni post-hoc.

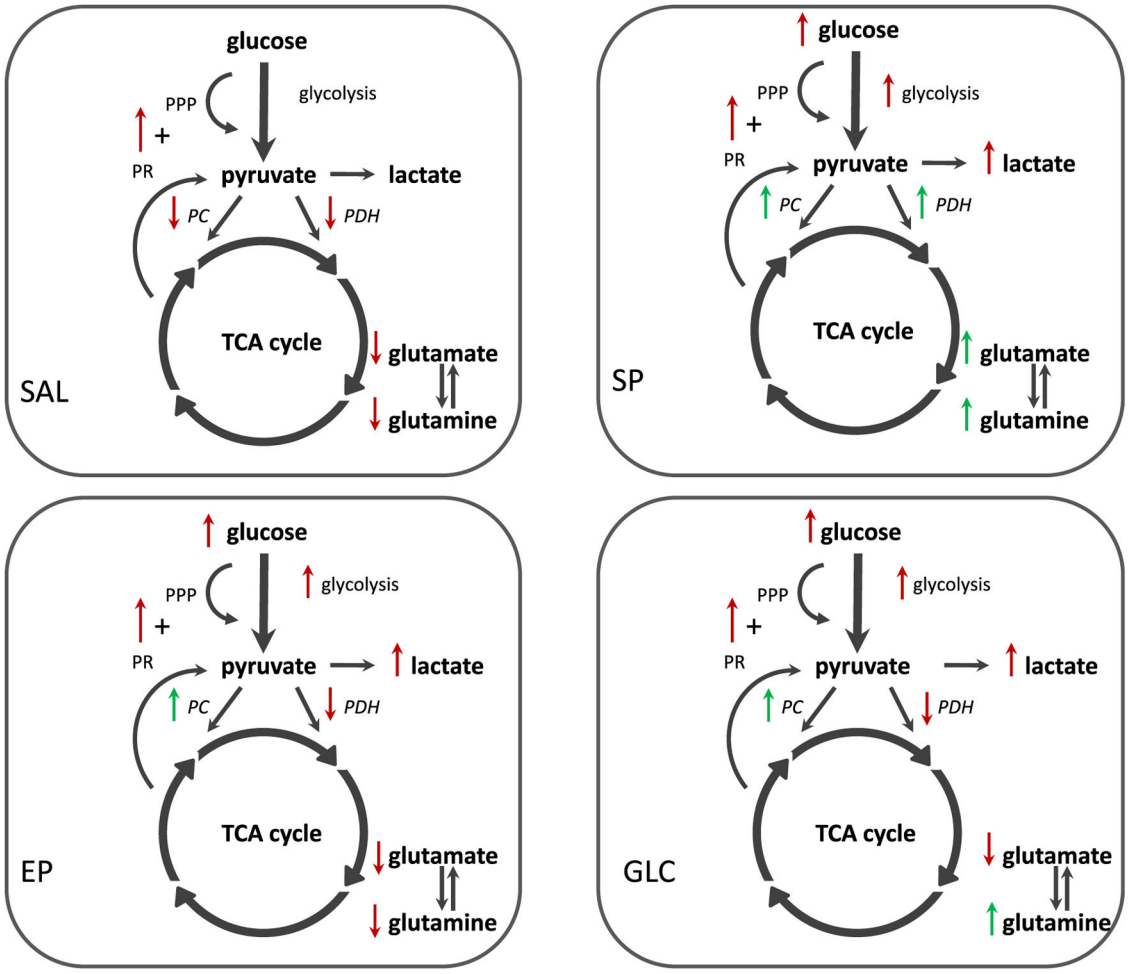

Fig. 4.

The overall changes in metabolite labeling in the first turn of the TCA cycle and the relative incorporation of ^{13}C label via different metabolic pathways in the injured cortex + hippocampus of CCI-injured animals following SAL or fuel treatment compared to Sham injury non-treated controls. In the SAL treated CCI-injured animals oxidative metabolism via both PC and PDH was reduced resulting in reduced ^{13}C labeling of glutamate and glutamine (red arrows). In addition, the relative contribution of the PPP + PR pathway to lactate labeling was increased (red arrow) although this did not significantly increase the ^{13}C lactate pool compared to Sham-controls. Following SP treatment, CCI-injured animals had increased lactate labeling via glycolysis and the PPP + PR pathway (red arrows). Glutamate and glutamine labeling via PDH and PC was similar to Sham-controls (green arrows) indicating improved neuronal and astrocyte metabolism compared to SAL. Similar to the SP group, EP treatment results in an increase in lactate labeling via glycolysis and the PPP + PR pathway (red arrows). However, oxidative metabolism via PDH was reduced (red arrows). In contrast, glutamate and glutamine labeling via PC was similar to Sham-controls (green arrow) suggesting improved astrocyte metabolism. With GLC treatment, ^{13}C label incorporation into lactate via the various metabolic pathways (red arrows) was similar to the pyruvate treatments. Oxidative metabolism via PDH resulted in reduced labeling of

glutamate (red arrows), however labeling of glutamine via PC was restored with GLC treatment (green arrows). Compared to SAL, the restoration of astrocyte-specific PC metabolism by SP, EP, and GLC treatment may underlie their abilities to improve cerebral glucose utilization and reduce neuronal loss following CCI injury. CCI, controlled cortical impact; EP, ethyl pyruvate; GLC, glucose; Lac, lactate; PC, pyruvate carboxylase; PDH, pyruvate dehydrogenase; PPP, pentose phosphate pathway; PR, pyruvate recycling; SAL, saline; SP, sodium pyruvate; TCA, tricarboxylic acid cycle.

Table 1

Arterial pH, blood gas, and plasma glucose and lactate concentrations.

		pH	HCO_3	pO_2	O_2 Sat	pCO_2	Glucose	Lactate
Sham *n* = 10	Pre	7.47 ± 0.01	27.01 ± 0.42	86.22 ± 1.64	97.16 ± 0.21	36.84 ± 0.83	10.18 ± 0.45	0.79 ± 0.13
	15 min	7.46 ± 0.01	26.35 ± 0.39	88.20 ± 2.52	97.16 ± 0.27	36.98 ± 0.82	14.40 ± 0.68	1.28 ± 0.10
	67 min	7.47 ± 0.01	26.98 ± 0.53	86.30 ± 2.11	97.03 ± 0.25	37.08 ± 1.01	12.81 ± 0.81	1.07 ± 0.14
CCI-SAL *n* = 9	Pre	7.46 ± 0.01	25.88 ± 0.25	84.33 ± 1.66	96.88 ± 0.20	36.37 ± 0.69	9.58 ± 0.45	**0.58 ± 0.03**¤
	15 min	7.46 ± 0.00	25.89 ± 0.29	86.11 ± 1.49	97.04 ± 0.17	36.62 ± 0.43	13.71 ± 0.41	0.93 ± 0.08
	67 min	7.47 ± 0.01	26.43 ± 0.58	86.22 ± 2.99	97.01 ± 0.38	36.38 ± 1.04	12.33 ± 0.52	0.96 ± 0.17
CCI-SP *n* = 10	Pre	**7.58 ± 0.01***^◦¤	**34.78 ± 1.07***^◦¤	84.00 ± 1.84	97.63 ± 0.18	37.02 ± 0.63	10.71 ± 0.53	0.94 ± 0.06
	15 min	**7.54 ± 0.01***^◦¤	**33.67 ± 1.01***^¤	84.80 ± 0.95	97.48 ± 0.07	39.31 ± 0.63	14.32 ± 0.54	**1.77 ± 0.15**◦
	67 min	**7.54 ± 0.01***^◦¤	**32.84 ± 0.85***^¤	84.10 ± 1.48	97.43 ± 0.12	38.19 ± 0.70	11.66 ± 0.52	1.40 ± 0.09
CCI-EP *n* = 9	Pre	7.48 ± 0.01	27.19 ± 0.32	84.78 ± 1.88	97.06 ± 0.21	36.67 ± 0.68	9.50 ± 0.29	0.66 ± 0.05
	15 min	7.48 ± 0.01	27.13 ± 0.33	89.33 ± 1.55	97.46 ± 0.17	36.78 ± 0.97	14.39 ± 0.47	1.19 ± 0.12
	67 min	7.48 ± 0.00	28.04 ± 0.45	85.44 ± 0.91	97.19 ± 0.09	37.51 ± 0.77	12.22 ± 0.71	0.92 ± 0.07
CCI-GLC *n* = 10	Pre	7.48 ± 0.01	27.61 ± 0.41	83.80 ± 1.76	96.98 ± 0.23	36.89 ± 0.70	11.74 ± 1.22	1.26 ± 0.28
	15 min	7.48 ± 0.01	26.96 ± 0.53	87.10 ± 1.58	97.36 ± 0.14	36.41 ± 0.97	16.14 ± 1.09	**1.76 ± 0.15**^◦
	67 min	7.48 ± 0.01	27.73 ± 0.53	86.10 ± 1.32	97.27 ± 0.16	36.76 ± 0.77	13.25 ± 0.90	1.24 ± 0.18

CCI, controlled cortical impact; EP, ethyl pyruvate; GLC, glucose; HCO_3, bicarbonate; O_2 Sat, oxygen saturation; pCO_2, partial pressure of carbon dioxide in mm Hg; pO_2, partial pressure of oxygen in mm Hg; SAL, saline; SP, sodium pyruvate.

The concentration of plasma glucose and lactate are expressed as mmol/L.

All values are expressed as mean ± SEM. Effects of Group (*p < 0.05 vs. Sham; ^ p < 0.05 vs. CCI–SAL; ‡ p < 0.05 vs. CCI–SP; ◦ p < 0.05 vs. CCI–EP, ¤ p < 0.05 vs. CCI–GLC) on pH, HCO_3, or lactate were evaluated using repeated measures one-way ANCOVA with Bonferroni post-hoc analysis and controlling for the effect of pre-infusion (Pre) pH, HCO_3, or lactate levels.

Group effects on pO_2, pCO_2, O_2 saturation, and glucose were evaluated using repeated measures one-way ANOVA with Bonferroni post-hoc analysis.

Table 2

The amount (nmol/mg protein) of ^{13}C labeled metabolites in the left cortex + hippocampus of Sham and injured cortex + hippocampus of CCI-SAL, CCI-SP, CCI-EP and CCI-GLC animals.

pathway	*label*	Sham *n* = 8	CCI-SAL *n* = 8	CCI-SP *n* = 8	CCI-EP *n* = 9	CCI-GLC *n* = 8
Lactate						
glycolysis	[2,3 $^{13}C_2$]	0.95 ± 0.05	1.44 ± 0.08	**2.78 ± 0.34** *^	**2.20 ± 0.20** *	**2.09 ± 0.10** *
PPP + PR	[3 ^{13}C]	0.08 ± 0.00	**0.23 ± 0.01** *	**0.24 ± 0.01** *	**0.24 ± 0.02** *	**0.25 ± 0.02** *
Glutamate						
PDH 1st turn	[4,5 $^{13}C_2$]	6.06 ± 0.21	**4.37 ± 0.27** *	5.04 ± 0.24	**4.73 ± 0.38** *	**3.87 ± 0.14** *ǂ
PDH 2nd turn	[1,2 $^{13}C_2$]	3.76 ± 0.36	**1.97 ± 0.11** *	**2.36 ± 0.20** *	**2.19 ± 0.19** *	**1.81 ± 0.09** *
PC 1st turn	[2,3 $^{13}C_2$]	3.13 ± 0.35	**1.69 ± 0.07** *	2.50 ± 0.16	2.56 ± 0.25	**1.99 ± 0.08** *
PPP + PR	[4 ^{13}C]	0.65 ± 0.04	**0.45 ± 0.03** *ǂ	0.82 ± 0.08	**0.47 ± 0.02** ǂ	**0.51 ± 0.03** ǂ
Glutamine						
PDH 1st turn	[4,5 $^{13}C_2$]	2.19 ± 0.10	**1.38 ± 0.11** *ǂ¤	2.13 ± 0.09	**1.58 ± 0.13** *ǂ	1.86 ± 0.11
PDH 2nd turn	[1,2 $^{13}C_2$]	1.68 ± 0.17	**0.69 ± 0.06** *	**1.04 ± 0.03** *	**0.71 ± 0.05** *	**0.88 ± 0.06** *
PC 1st turn	[2,3 $^{13}C_2$]	1.44 ± 0.15	**0.86 ± 0.07** *ǂ	1.52 ± 0.08	1.14 ± 0.12	1.14 ± 0.15
PPP + PR	[4 ^{13}C]	0.33 ± 0.03	0.25 ± 0.02	0.31 ± 0.01	0.31 ± 0.02	**0.35 ± 0.02** ^

CCI, controlled cortical impact; EP, ethyl pyruvate; GLC, glucose; PC, pyruvate carboxylase; PDH, pyruvate dehydrogenase; PPP, pentose phosphate pathway; PR, pyruvate recycling; SAL, saline; SP, sodium pyruvate.

The amount of ^{13}C labeled lactate, glutamate, and glutamine isotopomers was determined by ^{13}C NMR and expressed in nmol/mg protein.

All values are expressed as mean ± SEM.

* $p < 0.05$ vs. Sham;

^ $p < 0.05$ vs. CCI–SAL;

ǂ $p < 0.05$ vs. CCI–SP;

¤ $p < 0.05$ vs.

CCI–GLC using one-way ANOVA with Bonferroni post-hoc analysis.

Table 3

Estimates of the relative contribution of the PPP + PR pathway to lactate, glutamate and glutamine labeling and the PC/PDH ratio for glutamate and glutamine labeling in the left cortex + hippocampus samples of Sham and injured cortex + hippocampus of CCI-SAL, CCI-SP, CCI–EP and CCI-GLC groups.

	PPP + PR lactate	PPP + PR glutamate	PPP + PR glutamine	PC/PDH glutamate	PC/PDH glutamine
calculated as:	$\frac{[3\ \ 13C]Lac}{[2,3\ \ 13C2]Lac}$	$\frac{[4\ \ 13C]Glu}{[4,5\ \ 13C2]Glu}$	$\frac{[4\ \ 13C]Gln}{[4,5\ \ 13C2]Gln}$	$\frac{[2,3\ \ 13C]Glu}{[4,5\ \ 13C2]Glu}$	$\frac{[2,3\ \ 13C]Gln}{[4,5\ \ 13C2]Gln}$
Sham	9.2 ± 0.2	10.8 ± 0.7	17.6 ± 1.3	50.9 ± 4.4	65.8 ± 6.1
CCI-SAL	**16.8 ± 1.7** *ŧ◦¤	10.4 ± 0.7	20.5 ± 1.5	39.6 ± 2.5	64.6 ± 5.6
CCI–SP	8.9 ± 0.5	**15.8 ± 1.4** *^◦	15.0 ± 1.0	49.7 ± 2.5	71.6 ± 3.3
CCI-EP	10.8 ± 0.4	10.3 ± 0.8	17.2 ± 1.9	**54.2 ± 4.1** ^	68.0 ± 5.2
CCI-GLC	11.9 ± 0.6	13.5 ± 1.2	19. 8 ± 2.3	51.7 ± 2.3	52.9 ± 8.9

CCI, controlled cortical impact; EP, ethyl pyruvate; GLC, glucose; Gln, glutamine; Glu, glutamate; Lac, lactate; PC, pyruvate carboxylase; PDH, pyruvate dehydrogenase; PPP, pentose phosphate pathway; PR, pyruvate recycling; SAL, saline; SP, sodium pyruvate.

PPP + PR lactate is the contribution of the PPP + PR pathway to the labeling of lactate relative to glycolysis (in percent). PPP + PR glutamate and PPP + PR glutamine are the contribution of the PPP + PR pathway to the labeling of glutamate or glutamine relative to the amount of glutamate or glutamine labeled via PDH in the first turn of the TCA cycle (in percent). These values are the minimum value for these ratios and would be 1.5 fold higher when adjusted for differences in the number of labeled pyruvate molecules resulting from [1,2 $^{13}C_2$] glucose metabolism in the PPP (two) compared to the number of labeled pyruvate molecules resulting from the same number of [1,2 $^{13}C_2$] glucose molecules labeled in glycolysis (three; see Methods 2.10). The PC/PDH ratio is calculated as the amount of glutamate or glutamine labeled via PC relative to the amount of glutamate labeled via PDH in the first turn of the TCA cycle (in percent).

All values are expressed as mean ± SEM.

* $p < 0.05$ vs. Sham;

^ $p < 0.05$ vs. CCI–SAL;

ŧ $p < 0.05$ vs. CCI–SP;

◦ $p < 0.05$ vs. CCI–EP;

¤ $p < 0.05$ vs.

CCI–GLC using one-way ANOVA with Bonferroni post-hoc analysis.